Pergamon

Int. J. Heat Mass Transfer. Vol. 37, Suppl. 1, pp. 161–173, 1994

0017-9310/94 $6.00 + 0.00

0017-9310(93)E0066-P

An experimental study of critical heat flux in very high heat flux subcooled boiling

C. L. VANDERVORT
General Electric Company, Schenectady, NY 12345, U.S.A.

and

A. E. BERGLES and M. K. JENSEN
Department of Mechanical Engineering, Aeronautical Engineering and Mechanics, Rensselaer Polytechnic Institute, Troy, NY 12180-3590, U.S.A.

Abstract—An experimental study of forced convective subcooled boiling heat transfer to water was performed at heat fluxes that ranged beyond 10^8 W m^{-2}. One of the objectives of this study was to obtain predictive ability for the critical heat flux (CHF) at high heat fluxes. Experiments were performed with metallic tubes having inside diameters ranging from 0.3 to 2.7 mm. Mass fluxes ranged from 5000 to 40 000 kg m^{-2} s^{-1}, and exit subcoolings from 40 to 135°C. Exit pressures ranged from 0.2 to 2.2 MPa, and length-to-diameter ratios ranged from 2.0 to 50.0. Single-phase and two-phase pressure drop and heat transfer data were shown to be reasonably well predicted by existing correlations. Over 200 CHF stable data points were obtained. CHF was shown to be an increasing function of both mass flux and subcooling, and an inverse function of diameter. CHF increased for length-to-diameter ratios less than 10, and decreased with increasing exit pressure. Unreasonably low CHF values were obtained for several series of tests; these premature failures are believed to be the result of thermal-hydraulic or nucleation instabilities. A 'high flux' CHF data base containing over 700 data points was compiled, and a new statistical correlation was developed. This correlation was tested against a recently published data base, with an average deviation of 19.4%.

INTRODUCTION

SUBCOOLED forced convection boiling of water is recognized as one of the best means of accommodating very high heat fluxes. The critical heat flux (CHF) is the most important piece of thermal-hydraulic information required for design of cooling configurations for such systems as fusion reactor first walls and plasma limiters, fission research reactors, ion beam targets, high power electronic tubes, and rocket nozzles for high Mach number tunnels. These systems are modeled as constant heat flux, and the large increase in wall temperature at CHF usually results in cooling channel meltdown.

Boyd [1, 2], Koski and Croessmann [3, 4], and Wadkins *et al.* [5] describe the need to accommodate steady heat fluxes well above 10^7 W m^{-2} in this equipment. As demonstrated by Ornatskii and Vinyarskii [6], heat flux levels of 10^8 W m^{-2} are attainable through the use of high velocities, large subcoolings, small diameter channels, and short heated lengths. Through partial heating of the circumference and enhancement by means of a volatile additive, the highest recorded CHF of 3.5×10^8 W m^{-2} was obtained. In the present research program, CHF data were collected and assembled with previous data, so that a predictive correlation could be developed.

LITERATURE REVIEW

The critical heat flux condition in subcooled boiling of water has been investigated by numerous researchers. The first studies in small diameter tubes were those of Ornatskii and Kichigen [7], Ornatskii and Vinyarskii [8], and Bergles [9]. Available CHF data were first summarized by Loosmore and Skinner [10]. Review articles discussing CHF data and correlations in subcooled boiling have been presented by Gambill [11], Bergles [12], Boyd [13, 14], and Celata [15]. Recently, a new compilation of CHF data for both medium and high heat fluxes was published by Celata and Mariani [16].

EXPERIMENTAL FACILITY AND PROCEDURE

The following is a description of the experimental apparatus used for the subcooled boiling heat transfer experiments, and described in detail by Vandervort *et al.* [17]. Major components in the experimental loop, shown in Fig. 1, are: a diaphragm pump, preheaters, turbine flow meters, the test section, and a heat exchanger. The experiment was designed for a range of mass fluxes in small diameter tubes from 5000 to 50 000 kg m^{-2} s^{-1}, exit pressures from 0.1 to 2.2 MPa, subcoolings from 0 to 150°C, and length-to-diameter ratios of the primarily 304 stainless steel tubes from 1.0 to 100.0. Up to 100 kW of electric power was available, with maximum current up to 2500 A at 40 V. Temperature, pressure, and flow measuring instrumentation was installed. A Hewlett-Packard data acquisition system was assembled and software developed for processing of experimental data. The system was degassed until dissolved oxygen

NOMENCLATURE

A	heat transfer area [m^2]	ΔP_{adb}	pressure drop under adiabatic conditions [MPa]
D	inner diameter of test section [m]	(q/A)	heat flux [W m^{-2}]
G	mass flux [kg m^{-2} s^{-1}]	$(q/A)_c$	critical heat flux [W m^{-2}]
L	heated length of test section [m]	T	temperature [°C]
P	exit pressure or pressure level [MPa]	ΔT_{sub}	subcooling, $T_{sat} - T_b$ [°C].
ΔP	pressure drop [MPa]		

measurements indicated less than 1 cm^3 l^{-1} of dissolved gases. An ion exchanger maintained water purity at levels above 2 MΩ cm, as continuously monitored by a conductivity meter. Heat flux was defined by the electrical power input and the inner surface area. Uncertainties were estimated with a propagation-of-uncertainty analysis and are estimated to be: $q/(A)_c$, ±6.0%; G, ±7.9%; P, ±2.00%; ΔT_{sub}, ±6.9%; D, ±3.6%; L, ±3.7%.

RESULTS

Over two hundred stable CHF points were taken. Those points are listed in Table 1. Detailed parametric studies of the influence of mass flux, exit subcooling, diameter, and length-to-diameter ratio were performed. In addition, the influence of pressure, tube wall material, wall thickness, and dissolved gas content was explored. Parametric plots are presented of CHF vs each of these variables. In these plots, the non-varied parameters held constant are indicated and the maximum deviation from the 'constant' value is 10%, unless otherwise stated. For example, tests performed with an exit pressure of 0.6 MPa were allowed to range from 0.54 to 0.66 MPa. As a result, data scatter can be expected based upon the functional dependence between the measured CHF and the independent variables. Additional scatter results from experimental uncertainty, because some randomness may exist in the CHF phenomenon. Finally, because premature burnouts or unstable CHFs were experienced for an additional forty or so test sections, an effort was made to understand the conditions under which they occurred. Test sections were assumed to have failed

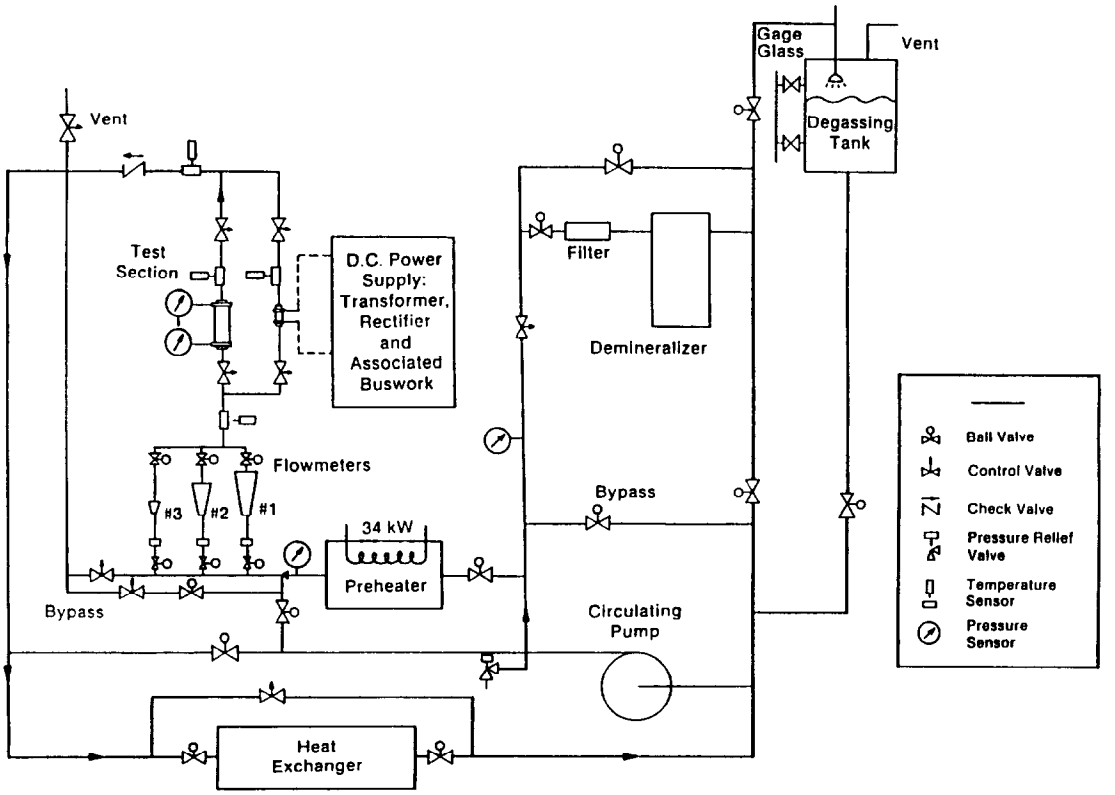

FIG. 1. Flow loop.

Table 1. RPI stable CHF data

#	D	(L/D)	P	G	ΔT_{sub}	$q/A \times 10^{-6}$	Mat.	Wall
1	2.016	25.65	0.202	9983	47.98	20.80	SS-304	0.579
2	2.016	25.65	0.198	19 751	50.42	22.60	SS-304	0.579
3	1.953	25.76	0.608	19 850	85.51	35.00	SS-304	0.611
4	2.057	24.58	1.230	25 349	98.12	49.33	SS-304	0.559
5	2.057	24.47	0.608	25 304	55.66	31.00	SS-304	0.559
6	2.057	24.55	0.605	24 921	52.45	30.90	SS-304	0.559
7	2.057	25.16	1.227	10 036	90.76	31.70	SS-304	0.559
8	2.057	25.20	0.607	25 437	98.16	49.40	SS-304	0.559
9	2.159	24.73	0.612	38 410	111.08	65.25	IN-600	0.508
10	2.159	24.85	0.597	10 340	55.69	21.95	IN-600	0.508
11	2.159	24.87	1.276	24 550	107.14	43.30	IN-600	0.508
12	2.667	24.90	0.600	24 450	101.25	4.60	IN-600	0.254
13	1.397	24.51	0.608	10 010	52.41	22.50	IN-600	0.889
14	1.397	24.78	0.628	41 785	106.91	82.20	IN-600	0.889
15	1.397	24.78	0.633	10 966	78.45	34.90	IN-600	0.889
16	2.440	24.68	1.218	9659	104.50	23.88	SS-304	0.304
17	2.440	24.79	0.597	24 130	101.70	40.61	SS-304	0.304
18	2.440	24.77	1.188	26 230	101.30	42.08	SS-304	0.304
19	2.440	24.79	0.606	39 831	107.60	69.48	SS-304	0.304
20	2.440	25.00	0.686	25 367	58.16	25.05	SS-304	0.304
21	2.440	25.00	0.569	25 863	95.78	41.29	SS-304	0.304
22	2.440	24.54	1.214	40 322	106.61	56.07	SS-304	0.304
23	2.440	24.54	1.227	40 334	107.81	55.29	SS-304	0.304
24	2.440	24.76	0.607	40 924	63.45	35.62	SS-304	0.304
25	1.803	23.67	0.608	24 986	95.08	45.30	SS-304	0.305
26	1.803	24.76	1.209	9885	105.04	23.50	SS-304	0.305
27	1.803	24.84	0.614	10 601	103.20	23.20	SS-304	0.305
28	1.803	24.68	1.232	24 591	100.58	40.60	SS-304	0.305
29	1.803	24.90	0.594	10 148	50.48	20.60	SS-304	0.305
30	1.803	24.85	1.211	9990	98.52	27.30	SS-304	0.305
31	1.803	24.83	0.602	26 070	53.40	30.70	SS-304	0.305
32	1.803	25.36	1.213	25 425	97.55	45.60	SS-304	0.305
33	1.803	25.46	0.577	24 964	50.35	30.70	SS-304	0.305
34	1.803	24.78	0.633	25 567	56.95	28.90	SS-304	0.305
35	1.803	24.74	0.634	25 414	100.28	54.40	SS-316	0.305
36	1.803	24.79	1.208	10 220	101.18	25.70	SS-316	0.305
37	1.803	24.85	0.597	39 000	107.07	70.40	SS-316	0.305
38	1.803	24.72	0.621	40 960	61.63	45.40	SS-316	0.305
39	1.803	24.79	1.231	41 810	101.91	67.40	SS-316	0.305
40	1.372	24.66	1.190	10 313	102.13	27.60	SS-304	0.229
41	1.372	24.63	1.172	25 165	100.07	36.20	SS-304	0.229
42	1.372	24.86	0.612	25 000	54.46	26.80	SS-304	0.229
43	1.372	24.84	0.614	10 119	57.75	18.70	SS-304	0.229
44	1.372	24.58	0.622	24 495	97.28	41.70	SS-304	0.229
45	1.372	24.71	1.205	10 110	97.34	29.40	SS-304	0.229
46	1.372	24.71	0.583	9749	53.42	21.10	SS-304	0.229
47	1.372	24.68	0.647	25 477	46.48	42.40	SS-304	0.229
48	1.372	24.57	1.225	24 980	103.16	49.80	SS-304	0.229
49	1.372	24.58	0.630	26 139	87.54	57.50	SS-304	0.229
50	1.372	24.06	0.623	9768	54.86	20.00	SS-304	0.229
51	1.372	24.02	0.629	40 418	102.39	82.90	SS-304	0.229
52	1.372	24.63	0.601	10 272	48.98	23.80	SS-304	0.229
53	1.372	24.93	0.686	37 700	65.31	51.00	SS-304	0.229
54	1.372	24.64	0.608	40 700	49.88	59.70	SS-304	0.229
55	1.067	23.98	0.193	12 205	31.51	19.00	SS-304	0.203
56	1.067	22.95	0.230	11 550	33.97	26.40	SS-304	0.203
57	1.067	25.06	0.220	13 253	41.64	31.20	SS-304	0.203
58	1.067	25.69	0.275	13 180	39.33	30.20	SS-304	0.203
59	1.067	26.21	0.221	13 703	48.81	29.90	SS-304	0.203
60	1.067	24.92	0.131	14 705	10.50	23.50	SS-304	0.203
61	1.067	23.87	0.169	13 957	48.88	32.70	SS-304	0.203
62	1.067	2.62	0.226	23 698	68.34	42.00	SS-304	0.203
63	1.067	2.54	0.216	9757	62.71	42.50	SS-304	0.203
64	1.067	1.66	0.216	9854	34.52	34.40	SS-304	0.203
65	1.067	23.25	0.629	9030	76.32	26.90	SS-304	0.203
66	1.067	24.45	0.614	8980	65.87	26.10	SS-304	0.203
67	1.067	24.43	0.624	8438	51.51	24.20	SS-304	0.203
68	1.067	24.76	1.216	10 292	89.22	33.40	SS-304	0.203
69	1.067	24.64	1.235	9842	58.95	21.10	SS-304	0.203

Table 1—*Continued*

#	D	(L/D)	P	G	ΔT_{sub}	$q/A \times 10^{-6}$	Mat.	Wall
70	1.067	24.78	1.216	9834	83.04	29.80	SS-304	0.203
71	1.067	24.56	1.207	10 191	67.93	25.20	SS-304	0.203
72	1.067	24.73	0.609	9854	53.61	24.80	SS-304	0.203
73	1.067	24.82	0.613	10 110	68.65	29.70	SS-304	0.203
74	1.067	24.77	0.667	25 000	93.13	49.90	SS-304	0.203
75	1.067	24.82	0.617	9860	38.43	21.80	SS-304	0.203
76	1.067	24.71	1.226	23 988	70.28	36.40	SS-304	0.203
77	1.067	24.77	1.291	25 795	08.50	52.00	SS-304	0.203
78	1.067	24.67	0.587	25 265	52.31	33.90	SS-304	0.203
79	1.067	24.79	0.615	25 184	76.89	45.80	SS-304	0.203
80	1.067	24.74	1.217	25 082	87.54	42.90	SS-304	0.203
81	1.067	24.73	1.203	25 117	112.70	55.40	SS-304	0.203
82	1.067	24.37	0.643	22 931	51.28	30.10	SS-304	0.203
83	1.067	24.37	0.674	24 102	58.32	33.80	SS-304	0.203
84	1.067	24.37	0.633	25 873	92.51	57.10	SS-304	0.203
85	1.067	24.69	0.629	10 552	75.09	30.80	SS-304	0.203
86	1.067	24.66	1.241	10 087	96.71	32.60	SS-304	0.203
87	1.067	24.67	1.242	25 818	117.70	59.80	SS-304	0.203
88	1.067	24.60	1.212	25 324	92.22	48.50	SS-304	0.203
89	1.067	24.98	0.596	25 196	60.48	34.00	SS-304	0.203
90	1.067	24.88	0.537	38 909	90.14	63.70	SS-304	0.203
91	1.067	24.88	0.582	41 155	101.24	83.10	SS-304	0.203
92	1.067	24.78	0.597	24 945	61.55	36.20	SS-304	0.203
93	1.067	23.77	1.232	40 280	130.40	88.40	SS-304	0.203
94	1.067	24.76	0.618	41 111	55.31	48.00	SS-304	0.203
95	1.067	25.03	0.603	40 080	86.30	62.80	SS-304	0.203
96	1.067	24.75	0.618	40 205	70.13	56.40	SS-304	0.203
97	1.067	25.23	1.202	40 120	76.52	59.60	SS-304	0.203
98	1.067	24.77	0.612	24 572	61.60	37.50	SS-304	0.203
99	1.067	24.78	0.597	24 945	61.55	36.20	SS-304	0.203
100	1.067	24.77	0.612	24 572	61.60	37.50	SS-304	0.203
101	1.067	24.78	0.597	24 945	61.55	36.20	SS-304	0.203
102	1.067	23.77	1.232	40 280	30.40	88.40	SS-304	0.203
103	1.067	24.76	0.618	41 111	55.31	48.00	SS-304	0.203
104	1.067	25.03	0.603	40 080	86.30	62.80	SS-304	0.203
105	1.067	24.75	0.618	40 205	70.13	56.40	SS-304	0.203
106	1.067	25.23	1.202	40 120	76.52	59.60	SS-304	0.203
107	1.067	25.03	0.583	41 190	98.10	87.00	SS-304	0.203
108	1.067	24.77	1.171	38 540	98.71	92.60	SS-304	0.203
109	1.067	25.18	0.616	25 525	98.61	56.80	SS-304	0.203
110	1.067	24.94	0.617	25 273	97.17	57.00	SS-304	0.203
111	1.067	24.76	0.620	24 902	99.53	55.00	SS-304	0.203
112	1.067	24.76	0.670	25 050	101.12	56.40	SS-304	0.203
113	1.067	24.76	0.665	24 684	99.20	56.70	SS-316	0.203
114	1.067	24.76	1.248	40 755	110.10	73.40	SS-316	0.203
115	1.067	24.95	0.608	25 270	103.20	51.50	SS-316	0.203
116	1.067	24.49	0.656	25 294	95.74	62.80	SS-316	0.203
117	1.067	24.87	1.227	41 307	90.58	74.40	SS-316	0.203
118	1.067	24.82	1.231	41 102	128.40	89.90	SS-316	0.203
119	1.067	24.64	0.600	40 408	55.49	51.20	SS-316	0.203
120	1.067	24.48	0.613	25 921	96.84	60.20	SS-316	0.203
121	1.067	24.77	0.620	39 845	57.10	49.80	SS-316	0.203
122	1.067	24.80	0.588	40 519	57.23	46.10	SS-316	0.203
123	1.067	24.84	0.752	25 403	52.45	37.40	SS-316	0.203
124	1.067	24.75	0.636	24 635	50.80	33.80	SS-316	0.203
125	1.067	24.84	0.408	25 861	52.39	34.30	SS-316	0.203
126	1.067	24.71	0.266	25 050	50.03	36.50	SS-316	0.203
127	1.067	24.84	0.136	25 614	53.00	35.50	SS-316	0.203
128	1.067	24.84	0.175	24 723	58.97	31.60	SS-316	0.203
129	1.067	24.18	0.831	25 348	97.41	59.00	SS-316	0.203
130	1.067	24.37	0.974	25 313	98.73	57.50	SS-316	0.203
131	1.067	24.56	1.582	24 858	108.51	49.20	SS-316	0.203
132	1.067	24.93	1.214	25 116	105.00	50.10	SS-316	0.203
133	1.067	24.93	1.392	24 625	105.00	50.70	SS-316	0.203
134	1.067	24.46	0.510	24 561	51.29	36.40	SS-316	0.203
135	1.067	24.75	2.052	24 751	97.93	49.20	SS-304	0.203
136	1.067	25.22	1.813	24 928	96.89	51.30	SS-304	0.203
137	1.067	24.56	2.277	5027	96.73	48.70	SS-304	0.203
138	1.067	2.16	1.227	25 064	100.90	63.50	SS-304	0.203
139	1.067	8.78	1.219	24 866	100.90	58.90	SS-304	0.203

Table 1—*Continued*

#	D	(L/D)	P	G	ΔT_{sub}	$q/A \times 10^{-6}$	Mat.	Wall
140	1.067	8.21	1.216	9791	94.62	36.40	SS-304	0.203
141	1.067	4.82	1.175	9952	107.40	35.30	SS-304	0.203
142	1.067	8.78	0.602	10 379	91.20	50.60	SS-304	0.203
143	1.067	19.92	1.208	25 070	115.10	59.50	SS-304	0.203
144	1.067	19.84	1.208	9837	101.40	33.00	SS-304	0.203
145	1.067	19.40	0.645	25 131	96.04	58.80	SS-304	0.203
146	1.067	14.60	1.214	9998	115.86	26.00	SS-304	0.203
147	1.067	15.00	1.244	25 095	102.11	56.30	SS-304	0.203
148	1.067	14.32	1.240	10 035	97.35	32.20	SS-304	0.203
149	1.067	9.87	1.211	25 096	116.33	54.50	SS-304	0.203
150	1.067	2.58	1.211	24 438	110.99	67.50	SS-304	0.203
151	1.067	2.71	1.205	10 101	108.91	44.80	SS-304	0.203
152	1.067	3.24	1.197	9878	108.17	42.20	SS-304	0.203
153	1.067	19.18	1.091	40 400	112.06	74.80	SS-304	0.203
154	1.067	15.02	1.246	40 190	107.02	79.10	SS-304	0.203
155	1.067	9.84	1.240	40 100	110.01	79.00	SS-304	0.203
156	1.067	4.27	1.244	24 504	114.32	66.00	SS-304	0.203
157	1.067	5.25	1.173	23 970	105.90	67.80	SS-304	0.203
158	1.067	2.36	1.221	39 420	104.20	85.70	SS-304	0.203
159	1.067	2.34	1.207	40 090	101.50	95.80	SS-304	0.203
160	1.067	9.93	1.221	10 079	103.10	36.90	SS-304	0.203
161	1.067	6.83	1.180	11 375	101.80	29.40	SS-304	0.203
162	1.067	9.47	1.235	24 678	104.70	61.10	SS-304	0.203
163	1.067	5.24	1.210	40 670	103.11	80.40	SS-304	0.203
164	1.067	4.78	1.234	39 590	104.54	80.20	SS-304	0.203
165	1.080	25.00	0.609	25 300	50.90	42.80	NI-200	0.254
166	1.080	24.67	0.610	24 540	51.90	43.80	NI-200	0.254
167	1.080	25.43	1.181	24 950	108.50	55.10	NI-200	0.254
168	1.080	24.78	1.196	24 460	80.62	42.10	IN-600	0.254
169	1.080	25.02	0.569	24 950	44.74	34.00	IN-600	0.254
170	1.080	24.82	0.458	24 006	65.52	40.50	IN-600	0.254
171	1.080	17.47	0.602	12 926	63.25	26.10	IN-600	0.254
172	0.775	18.10	1.197	13 567	100.32	47.30	IN-600	0.406
173	0.876	24.83	0.626	25 130	66.48	35.60	BRASS	0.356
174	0.876	25.22	0.612	24 800	63.00	33.20	BRASS	0.356
175	0.876	25.12	0.652	24 070	63.65	29.60	BRASS	0.356
176	0.686	23.00	0.668	26 010	89.14	61.60	SS-304	0.190
177	0.686	23.00	0.596	25 411	58.33	41.00	SS-304	0.190
178	0.686	21.00	0.604	10 355	59.09	26.20	SS-304	0.190
179	0.686	20.63	1.224	25 255	111.25	48.60	SS-304	0.190
180	0.686	22.68	0.612	9936	50.94	29.70	SS-304	0.190
181	0.686	22.42	1.208	24 943	100.99	53.40	SS-304	0.190
182	0.686	23.10	1.189	9671	98.23	30.50	SS-304	0.190
183	0.686	22.35	1.197	25 374	105.94	63.30	SS-304	0.190
184	0.686	23.01	0.586	41 361	101.90	85.80	SS-304	0.190
185	0.686	22.16	1.189	10 620	98.57	42.70	SS-304	0.190
186	0.686	23.04	0.611	10 080	58.61	29.00	SS-304	0.190
187	0.686	22.92	0.600	25 020	64.89	41.20	SS-304	0.190
188	0.686	23.10	0.611	24 500	54.78	42.90	SS-304	0.190
189	0.686	23.48	0.595	41 520	100.47	97.80	SS-304	0.190
190	0.508	21.12	1.188	25 251	110.69	61.10	SS-304	0.152
191	0.508	21.12	0.653	24 609	58.67	41.90	SS-304	0.152
192	0.508	21.12	0.618	25 070	55.17	46.60	SS-304	0.152
193	0.508	21.12	0.620	11 105	62.00	33.60	SS-304	0.152
194	0.508	21.57	1.180	24 721	110.21	56.50	SS-304	0.152
195	0.508	21.12	1.224	10 520	106.34	34.30	SS-304	0.152
196	0.508	21.36	1.217	10 214	99.62	31.42	SS-304	0.152
197	0.508	21.32	0.650	25 229	100.13	48.50	SS-304	0.152
198	0.508	21.65	0.583	41 250	97.14	94.10	SS-304	0.152
199	0.508	21.65	0.639	25 430	71.24	41.60	SS-304	0.152
200	0.508	21.65	0.605	40 038	56.98	61.40	SS-304	0.152
201	0.508	21.65	1.241	24 155	109.80	60.40	SS-304	0.152
202	0.508	21.65	1.226	40 113	113.90	78.70	SS-304	0.152
203	0.330	20.20	1.268	25 766	93.70	77.60	SS-304	0.152
204	0.330	19.99	1.227	24 860	105.70	80.40	SS-304	0.152
205	0.330	20.44	0.660	24 490	49.78	58.90	SS-304	0.152
206	0.330	20.59	0.551	10 685	50.00	35.70	SS-304	0.152
207	0.330	20.35	1.227	39 885	106.10	103.70	SS-304	0.152
208	0.330	21.20	0.564	25 085	58.38	54.00	SS-304	0.152
209	0.330	21.20	0.603	40 293	59.72	82.40	SS-304	0.152
210	0.330	21.20	0.672	39 463	90.34	123.80	SS-304	0.152

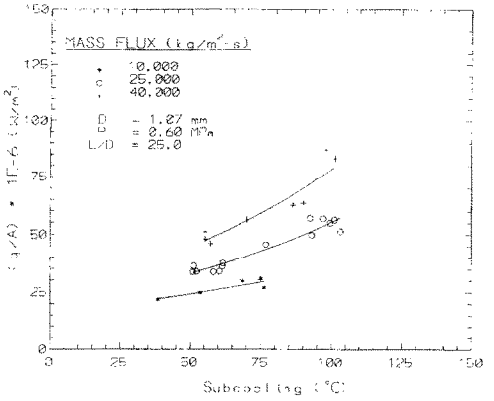

FIG. 2. CHF vs subcooling.

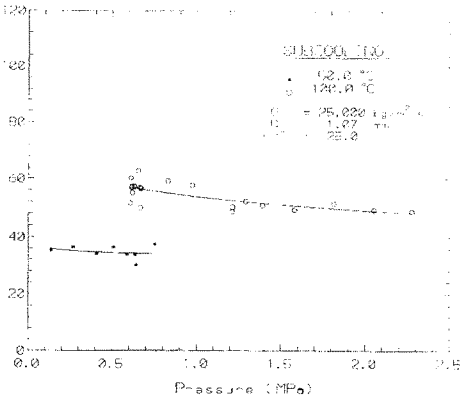

FIG. 4. CHF vs pressure.

prematurely if the point of failure was well upstream of the exit from the heated section.

The effects of exit subcooling and mass flux on CHF are shown in Fig. 2 for a pressure of 0.6 MPa. Least-square fits of the data were developed using the routines available with the plotting software. Experiments were performed for subcooling varying from 40 to 135°C, with mass fluxes of 10 000, 25 000, and 40 000 kg m^{-2} s^{-1}. The tube inside diameter was approximately 1.0 mm and the length-to-diameter ratio was 25. Under these conditions, CHF increased with subcooling, and the slope was an increasing function of the mass flux.

Figure 3 illustrates the dependence of CHF on tube inside diameter and mass flux, for a pressure of 0.6 MPa, length-to-diameter ratio of 25, and subcooling of 50°C. For each value of mass flux, CHF increased with decreasing diameter below 2.0 mm. CHF as a function of diameter and mass flux was also investigated at a subcooling of 100°C for pressures of 0.6 and 1.2 MPa. As observed by previous researchers, the magnitude of CHF increased with decreasing diameter. In contrast to these previous observations, the effect was most significant at the highest mass flux.

A series of experiments was performed in order to clarify the effect of pressure, with results shown in Fig. 4. Mass flux was held constant at 25 000 kg m^{-2} s^{-1}, diameter at 1.0 mm, and subcooling at 50 and 100°C. Virtually no pressure effect was noted; in fact, there seemed to be a very slight decrease of CHF with increasing pressure. This behavior agreed with the observations of Ornatskii and Vinyarskii [6].

The increase in CHF due to the reduction in length-to-diameter ratio is shown in Fig. 5 for an inside diameter of 1.0 mm, pressure of 1.2 MPa, subcooling of 100°C, and mass fluxes of 10 000, 25 000, and 40 000 kg m^{-2} s^{-1}. The effect seemed to be greatest for length-to-diameter ratios less than 10, indicating that CHF is related to the state of development of the flow regime.

Based on previous literature, it was reasonable to conclude that no effect of dissolved gas on CHF exists. However, slight uncertainty existed about the actual content of dissolved gas for these experiments, because continuous metering of the dissolved gas was not available. Discrete measurements indicated that the quantity was well below saturation values for water at room temperature and 0.1 MPa. For several data points, the dissolved oxygen concentration was measured with a hand-held Dissolved Oxygen Analyzer and found to be less than 2 p.p.m. corresponding to about 6 p.p.m. of dissolved air. A series of tests was performed with varying amounts of dissolved gas. Mass flux was set at 25 000 kg m^{-2} s^{-1},

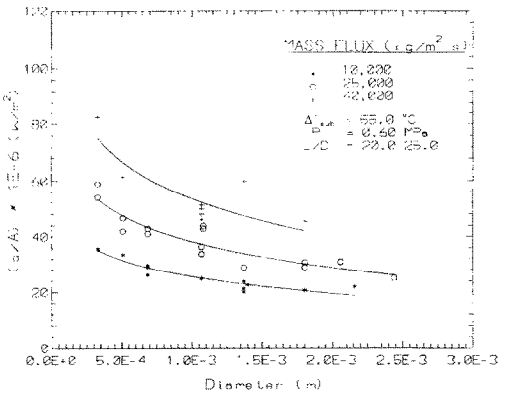

FIG. 3. CHF vs channel diameter.

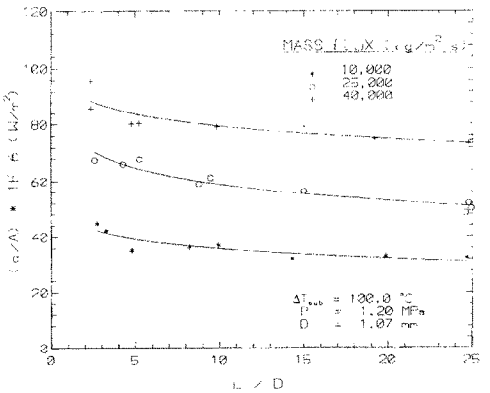

FIG. 5. CHF vs length-to-diameter ratio.

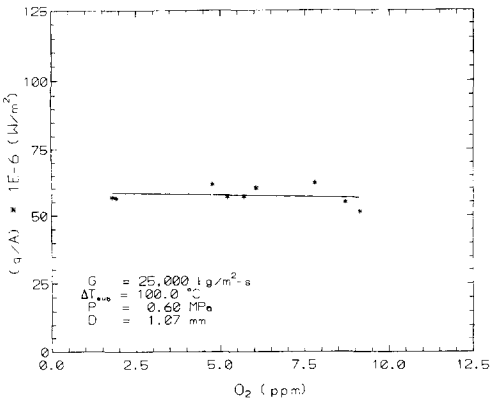

FIG. 6. CHF vs dissolved oxygen concentration.

pressure at 0.6 MPa, subcooling at 100°C, and inside diameter at 1.07 mm. No significant changes were observed in the CHF results over the range of dissolved gas concentration from near zero to the saturation level as shown in Fig. 6.

A number of researchers have questioned the effect of wall material or wall thermal properties on CHF. Five different materials were used in this study, stainless steel 304, stainless steel 316, nickel 200, brass (70/30), and Inconel 600. The MIT data, listed in ref. [12], were also taken with stainless steel 304. In comparison, most of the Soviet data were recorded with copper-alloy or nickel test sections. The majority of data of the present study were either stainless steel 304 or 316. Points were recorded for a mass flux of 25 000 kg m^{-2} s^{-1}, pressure of 0.6 MPa, subcooling of 100°C, and inside diameter of 1.07 mm (17 gauge) for each type of steel. No significant differences were noted. As test section diameter and, correspondingly, wall thickness were reduced, the current required to reach CHF became smaller. For test sections of less than 0.7 mm ID, current requirements were only a few hundred amperes and AC ripple became significant, raising questions in regard to the effect of AC vs DC heating. For several tests, a smaller 'pure' DC power supply was used. Data points for 0.33 and 0.51 mm diameter tubes were recorded with each power supply, with no significant differences noted.

One of the most interesting and perplexing aspects of this work was the persistent, often inexplicable occurrence of premature burnout. Table 2 is a log of all premature burnouts, complete with the conditions under which they occurred. At this point, premature burnout is defined as any thermal failure of the test section not directly attributable to CHF or some other obvious failure mechanism, such as procedural error. This statement requires an explanation. Figure 7 is a sketch of subcooled boiling pressure drop as a function of heat flux. This sketch is important in that the indicated line for increasing heat flux shows the path travelled during performance of the boiling curve and CHF experiments. It was possible to get these data because these premature failures occurred randomly for the indicated test sections. In addition, the pressure drop ratio was monitored whenever an inlet pressure tap was available.

The procedure for the CHF experiments followed a general pattern: flow parameters including mass flux, exit pressure, and inlet temperature were established with no energy input. This condition occurs at a heat flux ratio of zero, and a pressure drop ratio of 1.0. The power supply was turned on, and heat flux raised through the single-phase zone, where the pressure drop ratio decreased to near the minimum value. Nucleation began near the exit of the test section, counteracting the effect of increasing wall temperature in lowering the pressure drop ratio. The minimum was reached at a condition representing a trade-off between these effects. During boiling curve or diabatic pressure drop studies, the heat flux was raised in small increments so that conditions could be recorded. CHF tests typically began by raising the heat flux to a value of about 90% of the level required for incipient boiling based upon the Bergles and Rohsenow equation. Premature failures never occurred in the single-phase region. Entry into subcooled boiling was typically accompanied by 'boiling songs'; acoustic phenomena generally accompanied incipient boiling. Often, premature failure accompanied this traverse into nucleate boiling, the 'danger zone'. As stated, each of these failures occurred at an upstream location, as opposed to the tube exit where the lowest subcooling existed. Beginning near incipient boiling, the heat transfer became very sensitive; several test sections failed at this instant. Others failed at slightly higher heat flux levels, sometimes when power was being raised and occasionally under near steady-state conditions. Each test section that failed in this manner had some region of the tube that was experiencing incipient boiling. In general, once this region was traversed, the test sections were safe from premature failure and the heat flux was raised to the CHF level. Unfortunately, the region between incipient boiling and CHF is not large at high mass fluxes and subcoolings, causing this criterion to be rather subjective. As opposed to the premature failures, all reliable CHF data points occurred very near the test section exit.

The majority of premature failures occurred for two types of tubing, 1.8 and 2.4 mm diameter stainless steel capillary tubing. For these tubes, over two-thirds of all tests resulted in premature failure, with no discernible dependence on the five primary variables. No dependence upon mass flux, subcooling, or pressure was observed; failures occurred at each set of conditions for which these tubes were exposed. Each of these premature failures occurred at heat flux levels that were more than 20% below the CHF predicted by the present correlation.

Failure was always axially localized and nearly uniform around the circumference, as expected for a pressure drop oscillation, but different from that observed for a flow excursion. An inlet throttling valve was located immediately at the entrance of the test section

Table 2. Premature failures

#	D	(L/D)	P	G	ΔT_{sub}	$q/A \times 10^{-6}$	Mat.	ΔP_{sp}
1	2.440	49.20	1.14	9937	82.50	13.20	SS-304	2.80
2	2.440	48.90	0.611	19 294	53.50	21.70	SS-304	1.10
3	2.440	49.40	0.646	29 278	47.70	25.80	SS-304	0.58
4	2.440	24.80	1.186	10 025	122.50	16.10	SS-304	1.60
5	2.440	24.75	1.227	9987	111.70	18.90	SS-304	1.60
6	2.440	24.90	0.625	10 054	77.40	9.00	SS-304	2.20
7	2.440	24.79	1.192	10 281	126.40	13.30	SS-304	1.50
8	2.440	24.80	1.212	10 387	120.60	17.30	SS-304	1.30
9	2.440	24.76	0.586	10 014	60.90	8.70	SS-304	2.20
10	2.440	24.79	1.155	25 970	106.50	35.80	SS-304	1.90
11	2.440	24.71	1.188	25 490	109.20	30.90	SS-304	1.90
12	2.440	24.71	1.190	25 200	112.30	30.00	SS-304	1.90
13	2.440	24.80	0.590	25 065	60.50	22.10	SS-304	1.70
14	2.440	24.83	0.619	10 800	74.30	12.60	SS-304	1.80
15	2.440	24.79	1.241	25 760	111.80	27.50	SS-304	0.70
16	2.440	24.54	0.617	10 876	69.30	10.70	SS-304	0.70
17	2.440	24.84	0.629	24 781	51.50	21.40	SS-304	1.70
18	2.440	24.54	1.248	40 472	113.20	46.10	SS-304	0.70
19	2.440	24.55	0.607	38 378	64.00	31.20	SS-304	1.30
20	1.803	24.40	0.629	10 193	81.00	21.40	SS-304	0.73
21	1.803	24.70	1.210	25 400	106.90	30.70	SS-304	1.38
22	1.803	24.71	0.644	39 530	66.10	41.50	SS-304	1.12
23	1.803	24.36	0.629	25 833	60.80	24.60	SS-316	1.90
24	1.803	25.00	0.275	3068	40.40	8.60	SS-316	1.01
25	1.803	25.00	0.306	3059	51.20	7.52	SS-316	0.76
26	1.803	25.00	0.300	3281	53.70	7.80	SS-316	0.76
27	1.803	25.00	0.303	3356	55.20	7.70	SS-316	0.75
28	1.803	24.51	0.612	39 702	56.00	38.00	SS-316	0.76
29	1.067	24.79	0.624	25 261	61.60	20.70	SS-304	0.83
30	1.067	24.91	0.645	24 710	60.30	22.70	SS-304	0.85
31	1.067	24.56	1.622	25 324	122.50	32.60	SS-316	0.86
32	0.914	49.74	0.419	27 175	68.50	23.70	NI-200	0.74
33	0.914	49.60	0.524	9881	72.30	12.70	NI-200	1.52
34	0.914	49.78	0.615	10 475	61.70	17.10	NI-200	0.74
35	0.914	49.38	0.673	5625	40.40	11.60	NI-200	0.27
36	0.880	25.60	0.538	24 559	113.60	31.80	Brass	3.17
37	0.880	25.56	0.474	29 373	72.10	21.60	Brass	1.63
38	0.686	23.48	0.633	40 340	97.70	56.10	SS-304	0.79
39	0.508	21.65	0.635	24 840	115.00	25.10	SS-304	1.78
40	0.508	21.65	0.618	42 700	79.20	46.60	SS-304	1.24
41	0.508	21.65	0.603	41 229	68.00	51.60	SS-304	1.32
42	0.330	20.70	0.639	10 230	85.20	12.40	SS-304	1.50
43	0.330	20.70	1.162	25 702	141.90	35.10	SS-304	0.80
44	0.330	20.70	0.549	10 009	100.10	17.20	SS-304	1.53
45	0.330	19.30	0.642	10 374	103.35	18.10	SS-304	2.25

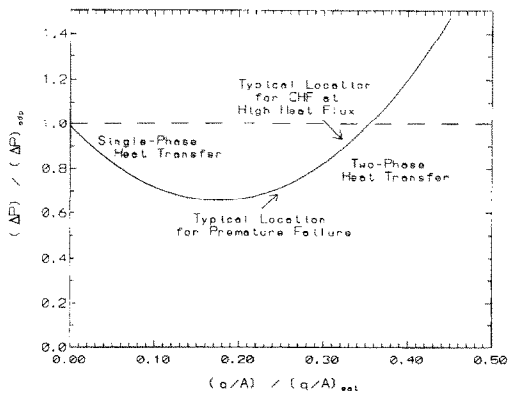

FIG. 7. Representation of premature failure phenomena.

so that a single-phase pressure drop of over 1.0 MPa existed immediately upstream of the test section. This value was determined by multiplying the single-phase pressure drop required to stabilize the flow, based upon the experimentally generated curves of this study, by at least a factor of five. Inlet pressure taps were drilled for only a few test sections, and premature failures occurred irrespective of their existence. It is unlikely that the pressure drop instability was the cause of premature failures, because of the relatively large inlet throttling that was used, and the very small compressible volume that existed between the inlet valve and the heated section.

Conversely, no premature failures were observed with the general purpose stainless steel and Inconel

tubes of inside diameter ranging from 1.4 to 2.7 mm, and, in particular, 2.1 mm. Only one difference was noted between these tubes and those observed to be susceptible to premature failure. Micro-roughness measurements revealed that the average roughness of the general purpose tubing was four times that of the capillary tubing, indicating that roughness may be a stabilizing factor.

These failures may be the result of some type of thermal-hydraulic phenomenon that occurs subsequent to incipient boiling. This statement is based upon the resemblance between the characteristics of these failures and those that have been observed due to the pressure drop instability. The 11 gauge (2.38 mm) and 13 gauge (1.80 mm) tubing were more susceptible to these types of failure because of their reduced thermal capacitance (thinner wall). Premature burnout may also have been the result of a spontaneous nucleation-type instability, though it is difficult to believe that nucleation can be suppressed for a water system. A few remarks are appropriate on this possibility. Under conditions of high velocity and heat flux, it can be shown that a relatively large level of superheat is necessary to initiate nucleation and for highly smooth surfaces, a shortage of nucleation sites could conceivably exist. Hence, under degassed conditions, it is possible that higher superheat is required for nucleation, though temperature 'overshoots' were not observed in the boiling curve studies. A metastable state can develop in which, given a small perturbation, a sudden, explosive formation of vapor may occur, which, in turn, can cause a momentary flow restriction that leads to premature failure.

The inconsistent performance of these tubes under conditions of high heat flux is a serious limitation for practical application of this technology. Cooling mechanisms at these high heat flux values seem to be somewhat fragile, and minor disturbances of the hydraulic, mechanical, or thermal state of the heat exchange device can cause sudden failure. It is important that these failure mechanisms be better understood and means made available for their suppression.

CORRELATION OF CHF DATA

Numerous types of CHF correlations have been proposed for subcooled forced convective boiling. The major types are empirical, similitude-based, analytical, tabular, and graphical. For the given range of experimental data upon which these correlations are based, CHF can usually be predicted with reasonable accuracy. Conversely, no correlations have been developed specifically for this regime, and a new correlation is needed. The 'high flux' region of boiling heat transfer is defined as the region encompassing a heat flux range from 10^7 to 2×10^8 W m^{-2}. For the purpose of this paper, data are included only for the region where decreasing diameter causes an increase in CHF, corresponding to diameters of less than 3.0 mm. The region where CHF reaches a local minimum vs subcooling was eliminated, by deleting all positive quality data and using data for mass fluxes greater than 3000 kg m^{-2} s^{-1}. Maximum pressure was limited to 3.0 MPa (450 psia), as this value is the present, approximate limit for which 'high-flux' applications exist.

In order to develop the correlation, a data base was needed. Several considerations governed the development and use of the data base. Data were assumed to be accurate and unbiased through systematic error. Projected correlational accuracy was determined by the experimental error of the data and could not suffer through systematic errors. As a safeguard against systematic error, large numbers of data attained through different sources were incorporated, and these data sets were assumed to be free of premature failures. Parametric trends, as described by the data, needed to be duplicated by the proposed correlation. Ideally, the data base will be uniformly distributed throughout the range of experimental parameters. An abundance of data for a single subrange would negate the influence of under-abundant data resident in other subranges. An example was the deletion of numerous CHF data for diameters over 3.0 mm.

Assembly of the 'high-flux' data base for uniformly heated, un-enhanced circular tubes was initiated by Loosmore and Skinner [10], who included the work of researchers from the MIT Heat Transfer Laboratory. A total of seven different researchers contributed over 200 applicable data points. Soviet data, that of Ornatskii [18], Ornatskii and Kichigan [7], and Ornatskii and Vinyarskii [8], were included. These data are particularly significant because these sets contain points recorded with the highest mass velocity, 90 000 kg m^{-2} s^{-1}, with resultant heat fluxes over 2×10^8 W m^{-2}. Several other researchers have since published in this area, but only Nariai *et al.* [19] and Boyd [20] have presented CHF data that could be included in the data base. The present data base now contains 721 data points, and the present correlation is developed from these data.

Numerous CHF correlations now exist in the general literature, the earliest of these CHF correlations were of the form

$$(q/A)_{cr} = A\,B^c\,D^e\,F^g,$$

where B, C, and F are the important variables or combinations of them, and A, c, e, and g are experimentally determined coefficient and exponents, respectively. An example of this type of correlation was that of Mirshak [21]. A second broad category of empirical correlations were based upon the 'superposition' principle. These correlations extended the Bergles and Rohsenow methodology for determination of forced convective, boiling heat transfer performance to CHF. An example of this form was the correlation of Gambill [22]. No influence of diameter or length was included, with the exception of the effect of diameter on the single-phase heat transfer coefficient. This type of correlation may prove suc-

cessful, as boiling curve studies demonstrate that as mass flux increases, the CHF level nears a lower limit set by the single-phase heat transfer. This anchoring to the single-phase contribution immediately focuses the correlation prediction within the correct order of magnitude. However, greater effort is required to model the boiling heat transfer contribution. Only one correlation was found for the high-flux region. This is the correlation by Shah [23, 24]. This correlation was applied to the data base because it included the early MIT data, and claims validity in the high-flux regime. Unfortunately, predictions with this correlation were poor, most data were under-predicted by up to 50%. In particular, the correlation does not reproduce the effect of reduced tube diameters.

In order to predict CHF at high heat fluxes, it was necessary to develop a new empirical correlation specifically for the high flux region. The statistical approach taken was to apply the CHF data base to an assumed model and minimize the squares of the residuals of the dependent variables. The analysis began by assuming that the data fit a general linear model [25]. A general purpose statistical program, SAS [26], was used with the RPI IBM 3081 mainframe computer. Five parameters, mass flux, exit subcooling, pressure, diameter, and length-to-diameter ratio are the predictor variables, with CHF the independent variable.

The first step of the process was to assume a log–linear relationship between CHF and each of the primary variables:

$$(q/A)_{cr} = A_0(G/G_0)^a(\Delta T_{sub})^b(P/P_0)^c \times (D/D_0)^e[(L/D)/(L/D)_0]^f$$

where

$$G_0 = 100\,000\ \mathrm{kg\,m^{-2}\,s^{-1}},$$
$$P_0 = 3.5\ \mathrm{MPa},$$
$$D_0 = 0.003\ \mathrm{m},$$
$$(L/D)_0 = 40,$$

and $(q/A)_{cr}$ is given in MW m^{-2}, and ΔT_{sub} is in °C. (Note: the letter 'd' was not used to avoid confusion later.) Regression was performed by taking the logarithm of this expression, giving

$$\log(q/A)_{cr} = \log(A_0) + a\log(G/G_0) + b\log(\Delta T_{sub}) + c\log(P/P_0) + e\log(D/D_0) + f\log[(L/D)/(L/D)_0].$$

Resultant predictive abilities were considered unsatisfactory. The resultant R^2 value was reasonable, 0.883, but significant cross-coupling effects between diameter, subcooling, and mass flux were neglected. In addition, the form of both the diameter and the length-to-diameter relationship were wrong. CHF asymptotically approached a lower limit for these variables, whereas the log–linear relationships predicted continuous lowering of CHF.

In order to include the cross-coupling of the independent variables, a more complex model was chosen:

$$(q/A)_{cr} = A_0(G')^{a_0+a_1G'+a_2T'+a_3P'+a_4D'+a_5(L/D)'} + (T')^{b_0+b_1G'+b_2T'+b_3P'+b_4D'+b_5(L/D)'} + (P')^{c_0+c_1G'+c_2T'+c_3P'+c_4D'+c_5(L/D)'} + (D')^{e_0+e_1G'+e_2T'+e_3P'+e_4D'+e_5(L/D)'} + (L/D)^{f_0+f_1G'+f_2T'+f_3P'+f_4D'+f_5(L/D)'}$$

where

$$G' = G/G_0 = G/10^5,$$
$$T' = \Delta T_{sub},$$
$$P' = P/P_0 = P/3.0,$$
$$D' = D/D_0 = D/0.003,$$
$$(L/D)' = (L/D)/(L/D)_0 = (L/D)/40.$$

The constants used here are also shown as part of a complete listing in Table 3. This new functional form significantly improved the predictive ability. The correlation coefficient increased to 0.9600. However, the parametric trends predicted for CHF as a function of both diameter and length-to-diameter ratio were incorrect. Experimental data indicated that CHF decreased to a limiting value for these variables, that of the infinitely long heated channel with moderate to large diameter. This opposed the mathematical limit enforced by the extended log–linear functional form.

Refinement began by addressing the length-to-diameter ratio effect. Very few data exist for (L/D) less than 15; included are early data of Bergles [9] and those of this study. Indicated trends demonstrated fairly weak couplings between (L/D) and the four remaining variables. Furthermore, scatter existed in the data, raising questions as to the true behavior. A

Table 3. Constants in CHF correlation

Constant	Value
G_0	10^5 kg m^{-2} s^{-1}
P_0	3.0 MPa
D_0	0.003 m
$(L/D)_0$	40.0
A_0	17.050
a_0	0.0732
a_4	0.2390
b_1	0.3060
b_2	0.0017
b_4	−0.0353
c_0	−0.1289
E_0	0.0121
e_0	−2.9460
e_1	0.7821
e_2	0.0093
F_0	1.5400
F_1	−1.2800

single fact was apparent: below (L/D) of approximately 15, the CHF increased with increasing (L/D). The trend could be approximated by the linear function proposed by Shah [23]. Then

$$f[(L/D')] = F_0 + F_1(L/D)',$$

with $F_0 = 1.54$, and $F_1 = -1.28$. This relationship was incorporated into the new correlation.

An improved form of the diameter effect was also assumed. The new form, with D' defined as before, is

$$f(D') = 1 + E_0(D')^{e_0 + e_1 G' + e_2 T' + e_3 P' + e_4 D' + e_5 (L/D)}.$$

Note that additional diameter dependence exists in the exponents for the other parametric variables. This fact and the complexity of the form prevented use of simple multiple linear regressive techniques, and it became necessary to use an iterative scheme. CHF level, divided by the assumed functional relationships for mass flux, subcooling, and pressure, was taken as the dependent variable in a new multiple regression analysis. This determined the values of E_0, e_1, e_2, e_3, e_4, and e_5. The CHF was then divided by the new functional form for the diameter effect. New values of A_0, a_1, a_3, ..., c_5 resulted from this linear regression model. Iterations were performed until negligible changes in these parameters resulted. Note that it was impossible to completely decouple the diameter effect from the other independent variables, because the quantity D' existed in the exponents of G', T', and P', and could not be conveniently divided out. The same complexity existed through the presence of G', T', and P' in the diameter expression.

Through these exercises, it became obvious that many of the correlational constants were unnecessary. Application of the statistical 't' test resulted in the elimination of the majority of the external parameters, with negligible effect on R^2. Three additional modifications were necessary in order to eliminate unphysical predictions for very low mass fluxes, subcoolings, and pressures. Small additive constants were included within the quantities G', T', and P'. Given these changes, the final correlation is

$$\begin{aligned}(q/A)_{cr} = {} & 17.05[(G')^{0.0732+0.2390(D')}] \\ & \times [(T')^{0.3060(G')+0.001730(T')-0.0353(D')}] \\ & \times [(P')^{-0.1289}] \\ & \times [1+0.01213(D')^{-2.946+0.7821(G')+0.009299(T')}] \\ & \times [1.540-1.280(L/D)'],\end{aligned}$$

where

$$\begin{aligned}G' &= 0.005 + G/10^5 \,(\mathrm{kg\,m^{-2}\,s^{-1}}),\\ T' &= 5 + \Delta T_{\mathrm{sub}}\,(^\circ\mathrm{C}),\\ P' &= (0.0333 + P)/3.0\,(\mathrm{MPa}),\\ D' &= D/0.003\,(\mathrm{m}),\\ (L/D)' &= (L/D)/40.\end{aligned}$$

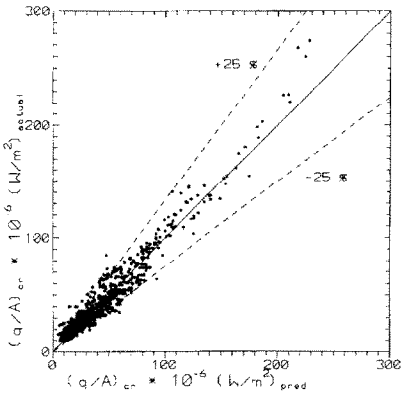

FIG. 8. Scatter plot for CHF correlation.

Each of the constants used for this correlation is listed in Table 3.

The resultant value of R^2 was now

$$R^2 = 0.9421,$$

slightly below the maximum value of 0.9600, obtained with 26 constants and non-physical behavior for diameter and length effects. Given that the data scatter exceeded 10%, this value was considered satisfactory. A scatter plot that compares the predicted CHF vs the Celata–Mariani high heat flux data from the data base in ref. [16] (891 points) is given as Fig. 8. The r.m.s. deviation was 19.4%.

Parametric plots were constructed that exhibit the predicted CHF levels as a function of each of the primary variables, with satisfactory results. In Fig. 9, predicted CHF is shown as a function of subcooling for values of mass flux varying discretely from 10 000 to 90 000 kg m^{-2} s^{-1}. Exit pressure was fixed at 1.2 MPa, diameter was fixed at 1.5 mm, and length-to-diameter ratio was fixed at 25.0. The behavior is similar to that observed in this study, as well as in previous studies; CHF increases with subcooling in a non-linear manner. CHF is plotted as a function of mass

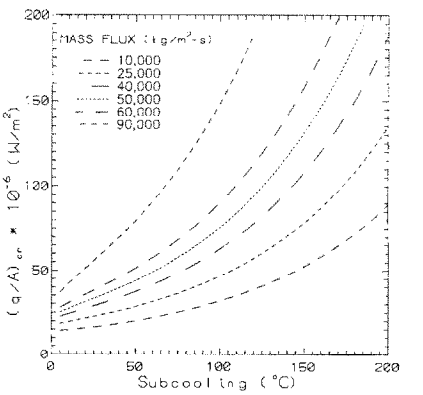

FIG. 9. Predicted CHF vs subcooling and mass flux.

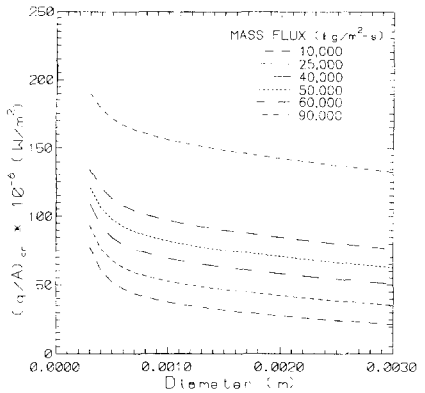

FIG. 10. Predicted CHF vs diameter and mass flux.

flux and diameter in Fig. 10, with an exit subcooling of 100°C, pressure of 1.2 MPa, and length-to-diameter ratio of 25.0. The CHF is shown to increase with decreasing diameter in a non-linear fashion. The predicted CHF is shown as a function of mass flux and pressure in Fig. 11.

SUMMARY AND CONCLUSIONS

An experimental apparatus was developed to perform forced convective, subcooled boiling heat transfer and pressure drop studies with small diameter tubes, ranging from 0.3 to 3.0 mm. Test sections were chosen to be lengths of metallic tubing, heated resistively. The experiment was designed to cover a wide range of operating and geometric parameters. Temperature, pressure, and flow measuring instrumentation was installed. Subcooled boiling CHF experiments were performed at heat fluxes ranging from 10^7 to above 10^8 W m^{-2}. Mass fluxes ranged from 5000 to 40 000 kg m^{-2} s^{-1}, and subcooling from 40 to 135°C. CHF increased with increasing subcooling and mass flux in a non-linear fashion. For exit pressures of 0.2 to 2.2 MPa, CHF was only weakly dependent on pressure, in that only a slight decrease in the CHF level was noted. Over a diameter range from 0.3 to 3.0 mm, CHF increased by a factor of two with decreasing diameter; the effect of decreased diameter was a function of mass flux and subcooling. The effect of length-to-diameter ratio was studied by performing experiments for values ranging from 1 to 25. Increases in CHF were only noted for length-to-diameter ratios less than 10. Experiments were also performed to understand the effect of varied dissolved gas concentrations on the CHF level. No influence was observed.

Throughout the CHF experiments, premature test section failures were observed. These failures occurred most often for 11 gauge (2.38 mm) and 13 gauge (1.80 mm) test sections. During all boiling curve studies and several CHF tests, failure was observed to occur near the tube location that was experiencing the onset of nucleate boiling. It is speculated that different nucleation behavior in these tubes results in a type of thermal-hydraulic or nucleation instability that exhibits characteristics similar to the pressure drop instability.

A data base of 'high-flux' CHF data was accumulated composed of over 700 points. Existing CHF correlations were applied to these data, with unsatisfactory predictive results. A new statistical correlation was developed, covering mass fluxes from 3000 to 90 000 kg m^{-2} s^{-1}, subcoolings from 0 to 200°C, pressures from 0.1 to 3.0 MPa, diameters from 0.3 to 3.0 mm, and length-to-diameter ratios from 1.0 to 40.0. Resulting CHF levels varied from 6×10^6 to 2×10^8 W m^{-2}. The revised correlation exhibits a mean deviation of about 19.4% when compared to the appropriate portion of the Celata–Mariani data base [16].

Acknowledgement—This study was supported in part by the U.S. Department of Energy under Grant No. DE-FG02-89ER14019.

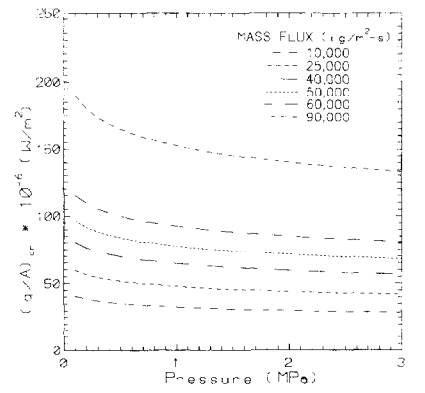

FIG. 11. Predicted CHF vs pressure and mass flux.

REFERENCES

1. R. D. Boyd, Heat transfer for fusion component applications, *Fusion Technol.* **13,** (1), 644–653 (1988).
2. R. D. Boyd, Critical heat flux and heat transfer transition for subcooled flow boiling, *J. Heat Transfer* **113,** 264–266 (1991).
3. J. A. Koski and C. D. Croessmann, Critical heat flux investigations for fusion-relevant conditions with the use of a rastered electron beam apparatus, ASME Paper No. 88-WA/NE-3 (1988).
4. J. A. Koski *et al.*, Thermal-hydraulic design issues and analysis for the ITER divertor, *Fusion Technol.* **19,** 1729–1735 (1991).
5. R. P. Wadkins, J. A. Lake and C. H. Oh, Heat transfer for the Ultra High Flux Reactor, A.I.Ch.E. Symposium Series, No. 275 **83,** 134–149 (1987).
6. A. P. Ornatskii and L. S. Vinyarskii, Critical heat transfer in the forced motion of underheated water–alcohol mixtures in tubes of diameter 0.5 mm, *Teplofizika Vysokikh Temperatur* (*High Temp.*) **3**(6), 881–883 (1965).
7. A. P. Ornatskii and A. M. Kichigan, Critical thermal

loads during the boiling of subcooled water in small diameter tubes, *Teploenergetika* **6**, 75–79 (1962).
8. A. P. Ornatskii and L. S. Vinyarskii, Heat transfer crisis in a forced flow of underheated water in small bore tubes, *Teplofizika Vysokikh Temperatur* (*High Temp.*) **3**(3), 444–451 (1964).
9. A. E. Bergles, Subcooled burnout in tubes of small diameter, ASME Paper No. 63-WA-182 (1963).
10. C. S. Loosmore and B. C. Skinner, Subcooled critical heat flux for water in round tubes, S. M. Thesis, Massachusetts Institute of Technology, June (1965).
11. W. R. Gambill, Burnout in boiling heat transfer—Part II: Subcooled forced convection systems, *Nucl. Safety* **9**(6), 47–65 (1968).
12. A. E. Bergles, Burnout in boiling heat transfer–Part II: Subcooled and low-quality forced-convection systems, *Nucl. Safety* **18**(2), 154–167 (1977).
13. R. D. Boyd, Subcooled flow boiling critical heat flux (CHF) and its application to fusion energy components. Part I: Fundamentals of CHF and related data base, *Fusion Technol.* **7**(1), 19–30 (1985).
14. R. D. Boyd, Review of subcooled flow boiling critical heat flux (CHF) and its application to fusion systems. Part II: A review of microconvective, experimental and correlational aspects, *Fusion Technol.* **7**(1), 31–42 (1985).
15. G. P. Celata, A review of recent experiments and predictive aspects of burnout at very high heat fluxes, *Proc. of the International Conference on Multiphase Flow*, p. 191 Tsukuba, Tsukuba, Japan, 24–27 Sept. (1991).
16. G. P. Celata and A. Mariani, A data set of critical heat flux in water subcooled flow boiling, *Specialists' Workshop on the Thermal-Hydraulics of High Heat Flux Components in Fusion Reactors*, Coordinated by G. R. Celata and A. Mariani, ENEA-C.R.E. Casaccia, Italy, (1993).
17. C. L. Vandervort, A. E. Bergles and M. K. Jensen, The ultimate limits of forced convective heat transfer, Rensselaer Polytechnic Institute Report HTL-9, Troy, NY (1992).
18. A. P. Ornatskii, The influence of length and tube diameter on critical heat flux for water with forced convection and subcooling, *Teploenergetika* **7**(6), 67–69 (1960).
19. H. Nariai, F. Inasaka and T. Shimura, Critical heat flux of subcooled boiling in narrow tubes, *Proc. of the* 1987 *ASME–JSME Thermal Engineering Joint Conference*, Vol. 5, pp. 455–462. Hemisphere, New York (1987).
20. R. D. Boyd, Subcooled water flow boiling at 1.66 MPa under uniform high heat flux conditions, *Fusion Technol.* **16**(5), 324–330 (1989).
21. S. Mirshak, W. S. Durant and R. H. Towell, Heat flux at burnout, Savannah River Laboratory Report No. DP-355 (February 1959).
22. W. R. Gambill, Generalized prediction of burnout heat flux for flowing, subcooled, wetting liquids, *A.I.Ch.E. Symposium Series*, No. 41, Vol. 59, pp. 71–87 (1962).
23. M. M. Shah, A generalized graphical method for predicting CHF in uniformly heated vertical tubes, *Int. J. Heat Mass Transfer* **22**, 557–568 (1979).
24. M. M. Shah, Improved general correlation for critical heat flux during upflow in uniformly heated vertical tubes, *Int. J. Heat Fluid Flow* **8**(4), 326–335 (Dec. 1987).
25. B. L. Bowerman, R. T. O'Connel and D. A. Dickey, *Linear Statistical Models: An Applied Approach*. Duxbury, Boston, MA (1986).
26. SAS Institute Inc., *SAS User's Guide: Statistics*, Version 5th Edition. SAS Institute Inc., Cary, NC (1985).